Ionic Strength Dependence of Protein-Polyelectrolyte Interactions

Emek Seyrek,[†] Paul L. Dubin,*[,†] Christophe Tribet,*[,‡] and Elizabeth A. Gamble[†]

Department of Chemistry, Indiana University-Purdue University at Indianapolis, 402 N. Blackford Street, Indianapolis, Indiana 46202, and Laboratoire de Physico-Chimie des Polymères, UMR CNRS 7615, ESPCI, Université Paris 6, 10 rue Vauquelin, 75231 Paris Cedex 05, France

Received September 3, 2002; Revised Manuscript Received October 25, 2002

The effect of univalent electrolyte concentration on protein-polyelectrolyte complex formation has been measured by frontal analysis continuous capillary electrophoresis (FACCE) and turbidimetry for the interaction of bovine serum albumin (BSA) with a synthetic hydrophobically modified polyacid, for BSA with (porcine mucosal) heparin (Hp), a highly charged polyanion, and for Hp and insulin. All three highly diverse systems display maxima or plateaus in complex formation in the range of ionic strength $5 < I < 30$ mM, confirmed in the case of BSA-Hp by multiple techniques. Similar maxima are reported in the literature, but with little discussion, for BSA-poly(dimethyldiallylammonium chloride), lysozyme-hyaluronic acid, and lysozyme-chondroitin sulfate, always in the I range 5−30 mM. While inversion of salt effect has been discussed specifically for the interaction of gelatin and sodium polystyrenesulfonate with gelatin[28] and with β-lactoglobulin,[10] the general nature of this phenomenon, regardless of polyelectrolyte origin, molecular weight, and charge sign has not been recognized. The position of the maxima and their occurrence when protein and polyelectrolyte have the same net charge imply that they arise when Debye lengths extend, at low I, beyond half the protein diameter so that addition of salt screens repulsions, as well as attractions. This appears to be a general effect caused by electrostatic repulsions that can coexist simultaneously with hydrophobic interactions. Modeling of protein electrostatics via Delphi is used to visualize this effect for BSA, lysozyme, insulin, and β-lactoglobulin.

Introduction

Proteins interact strongly with both biological and synthetic polyelectrolytes, but despite the fundamental similarities of both phenomena, the two fields of investigation are virtually isolated from each other. In the realm of biochemistry and biophysics, the dominant theme is that of DNA-binding proteins. Interactions of synthetic polyelectrolytes and proteins, on the other hand, have been studied in such technological contexts as enzyme immobilization,[1] protein separations,[2] sensor development,[3] and stimuli-responsive systems.[4] There is some logic in this scientific compartmentalization, in that the former phenomena correspond to the high-affinity binding, selective recognition, and high specificity essential to those protein functions that involve of necessity configurational precision. The latter, in contradistinction, involving noncognates (even when both species are of biological origin), typically are considered to present cases of "loose", nonspecific, low-affinity, nonselective binding. The borderline between these two fields may become more diffuse because of the growing focus on glycosamingoglycans (GAGs), biological strong polyelectrolytes with notably little secondary or tertiary structure, which approximate much more closely the statistical chain features of synthetic polyelectrolytes and of which the complex and manifold biochemical roles apparently involve, to a large extent, protein binding. Given the configurational flexibility of GAGs such as heparin (Hp) and heparan sulfate, conceptual models involving a single, well-defined protein-ligand structure may be less unassailable, and insights gained from noncognate systems may be more relevant to cell biology.

In all of the preceding examples, ionic strength and counterions strongly modulate the affinity between the macromolecules. Starting from Manning's fundamental treatment of counterion condensation,[5] Record and co-workers provided a general treatment of this effect that focused on DNA interactions with oligopeptides and proteins.[6] The experimental cornerstone of this approach has been measurement of the ionic strength dependence of the binding constant. The results are generally expressed by the "Record-Lohman" equation:

$$\log K_{obs} = \log K^0 - Z\varphi \log [M^+] \qquad (1)$$

Here, K^0 is the equilibrium constant for the reaction L + D = L−D + $Z\varphi(M^+)$, where L is the oligopeptide, D is DNA, Z is the ligand charge, and φ is the fraction of counterion (M^+) thermodynamically associated with the polyelectrolyte. The equation predicts a monotonic (double logarithmic) dependence of the binding constant on the ionic strength and has been used to identify the DNA-binding sites for various polypeptides and oligopeptides[7,8] with results that have been

* To whom correspondence should be addressed. E-mail addresses: dubin@chem.iupui.edu; Christophe.Tribet@espci.fr.

[†] Indiana University−Purdue University at Indianapolis.

[‡] Université Paris 6.

10.1021/bm025664a CCC: $25.00
Published on Web 01/25/2003

compared favorably in many cases to crystallographic data. Therefore, it is interesting to note several recent reports of nonmonotonic ionic strength dependence of the binding constant for protein-polyelectrolyte systems. Maxima in protein-polyelectrolyte affinity as a function of added salt were observed for systems as diverse as lysozyme/chondroitin sulfate and lysozyme/hyaluronic acid,[9] and beta-lactoglobulin (BLG)/sodium polystyrenesulfonate,[10] interestingly all in the same ionic strength range of 10−30 mM. Marky and Manning have also theoretically examined a nonmonotonic ionic strength behavior of binding of λ repressor protein and DNA.[11] The influence of ionic strength on protein-polyelectrolyte complexation was also recently examined for the case of lysozyme and polyanions by Monte Carlo simulations.[12]

The goal of the present work is to establish whether these observations are unrelated or anomalous or both or whether they represent some more general phenomenon. To do so, we have intentionally chosen highly divergent systems: heparin-bovine serum albumin, heparin-insulin, and bovine serum albumin with hydrophobically modified poly(acrylic acid) (HMPAA). These examples include both large and small proteins, a predominantly hydrophilic and highly charged glycosaminoglycan, and polymers of both high and low molecular weights. We have chosen to include HMPAA to explore how and whether the ionic strength effect in question is manifested in the presence of strong, localized apolar interactions. A common observation of the existence of an optimal salt concentration for the binding for a wide range of biopolymeric and semi-abiotic systems would clearly require an explanation that goes beyond consideration of specific geometry at the binding site. Because a special effect in the low ionic strength range could be related to long-range interactions (10−30 mM salt corresponding to Debye lengths of 2−4 nm), we have computed electrostatic potentials around these proteins to visualize their electrostatic anisotropy. The goal of this and related further studies is thus to establish the structural parameters that dictate the coexistence and consequences of concomitant repulsions and attractions of electrostatic origin in protein/polyelectrolyte association.

Experimental Section

Materials. Heparin (Hp) (sodium salt, porcine intestinal mucosa, lot B35123, nominal MW 14 kD) and insulin (0.67% zinc, porcine, lot B34749, MW ca. 3.0 kD) were purchased from Calbiochem (La Jolla, CA). Bovine serum albumin (BSA) (fatty acid free, lot 85155438, MW 68 kD) was from Boehringer Mannheim Corp. (Indianapolis, IN). All other reagents were from Fisher Scientific at the highest available purity. All solutions were prepared with Milli-Q water (Millipore, Milford, MA).

Hydrophobically modified poly(acrylic acid)s (HMPAA) were synthesized by grafting two poly(acrylic acid) precursors (Polysciences Inc,Warrington, PA) having nominal molecular weights of 150 000 and 5000 g mol^{-1}. Analyses by size exclusion chromatography performed in 0.5 M $LiNO_3$ gave corresponding number-average molecular weights of 130 000 and 5000 g mol^{-1} and polydispersity indices of 4 and 2, respectively. A minor fraction of the acid groups were grafted by an octyl- or octyldecylamine to yield the random HMPAA copolymers. The designation of each copolymer indicates its MW and grafting degree as determined by ^{1}H NMR, "150-3c18" thus corresponding to 3 mol % octadecane and MW 150 000.

Turbidimetric Titration. Turbidity measurements were used to determine the pH of initial complex formation (pH_c) at various ionic strengths.[10,13] The turbidity, reported as 100-%T, was measured ($\pm$0.2%T) with a Brinkman PC 800 probe colorimeter at 420 nm equipped with a 1 cm path length probe and calibrated to 100% transmittance with Milli-Q water. The pH was measured with an Orion 811 pH meter equipped with a Beckman refillable combination pH electrode and calibrated with pH 7 and pH 4 buffers. Hp and BSA solutions were prepared in the appropriate salt solution, allowed to stir for at least 1 h, and filtered (Whatman 0.45 μm) prior to use. A solution containing 1 g/L of BSA and 0.1 g/L of Hp was adjusted to an approximate pH of 8.5 with 0.1 N NaOH. The turbidity of the solution was measured as a function of pH by titrating with 0.1 N HCl with gentle magnetic stirring. For turbidimetric measurements with insulin-Hp, protein solutions prepared in the appropriate salt medium were adjusted to an approximate pH of 10.5 and allowed to stir for at least 1 h, combined with insulin stock solution to give 0.1 g/L of insulin and 0.01 g/L of Hp, adjusted to pH ca. 9.5, and titrated as above.

Dynamic Light Scattering. Dynamic light scattering (DLS) was performed to verify pH_c values determined via turbidity measurements. Samples were filtered (0.1 μm Whatman) and analyzed with a DynaPro 801 DLS instrument (Protein Solutions, Inc) equipped with a 30 mW solid-state 790 nm laser. The intensity of the scattered light was detected by an avalanche photodiode detector at 90° scattering angle. The mean apparent translational diffusion coefficient (D_T) was calculated by fitting the autocorrelation function using cumulants method. The hydrodynamic radius (R_h) of the particles was determined from the Stokes-Einstein equation

$$R_h = \frac{k_b T}{6\pi\eta D_T} \tag{2}$$

where k_b is the Boltzmann's constant, T is the temperature in K, and η is the solvent viscosity. "pH_c" was determined as the point at which both the scattering intensity and R_h initially increased.

Frontal Analysis Continuous Capillary Electrophoresis (FACCE). Capillary electrophoresis for BSA-Hp was performed at IUPUI using a P/ACE 5500 CE (Beckman Instruments, Fullerton, CA) with 214 UV detection operating at 5 kV and 25 °C with fused silica capillary (Polymicro Technologies Inc., Phoenix, AZ) of dimensions 50 μm × 27 cm (effective length 20 cm). Sample solutions were made from freshly prepared stock solutions of BSA and Hp dissolved in the CE phosphate run buffer adjusted to appropriate pH and ionic strength. The concentration range for BSA was 1.2−8.0 g/L, and Hp concentration was constant at 0.2 g/L. FACCE experiments were performed as

explained previously[14] at pH 6.8 to obtain the binding at ionic strengths 0.002, 0.007, 0.01, 0.03, and 0.05 M.

Capillary electrophoresis experiments with BSA and HMPAA were performed at ESPCI with a Beckmann P/ACE MDQ system equipped with a diode-array detector for simultaneous detection at two wavelengths (usually 205 nm and 280 nm). The bare silica capillaries (J & W Scientific) were 75 μm i.d. × 60 cm or 20 μm i.d. × 31 cm depending on the ionic strength of the run buffer, which was 2.5−400 mM, pH 9.2, boric acid-NaOH. Capillaries were flushed daily with 0.1 M NaOH, rinsed with water, and equilibrated with run buffer. Polymer (HMPAA 5-3C18, 5-5C8, or 150-3C18) was dissolved in water at 1 wt % for at least 18 h. BSA (5 wt %, Sigma, fraction V) was dialyzed overnight against 5 or 40 mM, pH 9.2, boric acid-NaOH buffer. HMPAA and BSA solutions were mixed at least 2 h before FACCE, though 2−3 day old samples gave the same results as freshly prepared ones (10−20 min). Polymer and protein final concentrations were varied from 0.01 to 0.1 wt % and from 0.1 to 1 wt %, respectively, to get binding isotherms over 2 decades in free BSA concentrations (for details, see ref 14). Variation of ionic strength at fixed total macromolecular compositions was achieved as follows. Polymer stock solution, dialyzed BSA, and boric acid-NaOH buffer were incubated for 2 h to give 2.5 or 5 mM borate. Eight or ten 350-μL aliquots of this master solution were each combined with 50 μL of Borax buffer of varying concentrations. The final polymer concentration was typically 0.02 wt %, and the BSA concentration ranged from 0.1 to 0.4 wt % as determined by the master solution. FACCE was carried out after 2-h incubation using a run buffer with the same borate concentration as the sample.

Computational Methods. Computer modeling facilitates the explanation of the effect of salt concentration and pH by allowing the visualization of the electrostatic potential around the protein as a function of pH and ionic strength. The potential was calculated by nonlinear solution to the Poisson-Boltzmann equation via Delphi version 98.0. The protein crystal structures with Protein Data Bank identifications 1AO6 (BSA), 132L (lysozyme), 1APH (insulin), and 1BSY (BLG) were taken from RCSB Protein Data Bank (http://www.rcsb.org). The charges of amino acids on the proteins were determined using the spherical-smeared-charged model put forward by Tanford,[15] utilizing the protein titrations curves of each protein[16−19] as explained previously.[14]

Results

Turbidimetric titrations and dynamic light scattering experiments were performed with mixtures of BSA and Hp at various ionic strengths to obtain qualitative information about the interaction of BSA and Hp. A typical result for the two techniques is given in Figure 1. Turbidity, total intensity, and measurement of apparent mean Stokes radius all reveal three domains of pH corresponding to (1) the absence of interaction, (2) soluble complex formation, and (3) phase separation of an insoluble complex.[12] The transition from region 1 to region 2 is denoted "pH_c". Changes in transmittance, total intensity, and R_h all result from the enhancement of particle mass upon complexation and, consequently, yield identical values of pH_c at all ionic strengths studied.

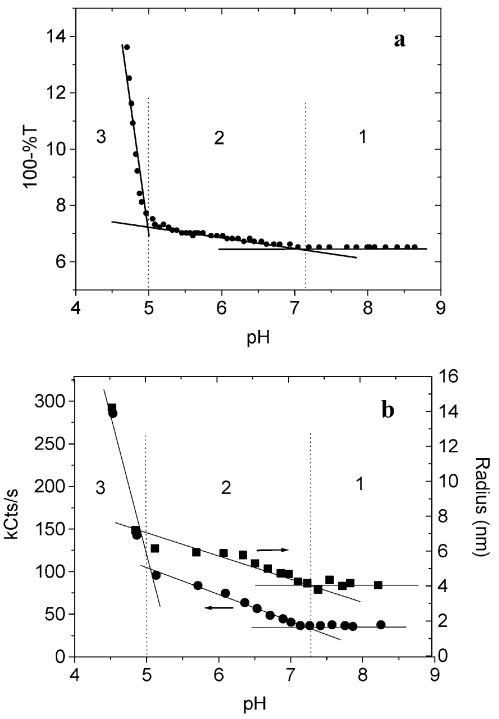

Figure 1. Turbidimetric titration curve (a) at $I = 10$ mM for 1 g/L of BSA with 0.1 g/L of Hp and pH dependence (b) of (●) total count rate and (■) apparent mean Stokes radius from DLS with BSA (1 g/L) and Hp (0.1 g/L) in 10 mM NaCl.

A plot of pH_c vs ionic strength for BSA-Hp (Figure 2a) may be viewed as a phase boundary in that it defines conditions under which complexation does not occur ($pH > pH_c$). Above 10 mM NaCl, pH_c decreases with increasing ionic strength, as expected because of the diminution of binding energy upon shielding between the charges on Hp and the protein's locally positive domain. However, the effect of ionic strength vanishes at lower salt concentrations. The result for insulin-Hp (Figure 2b) is even more dramatic because a maximum in binding (onset of complexation at the highest pH) appears at 30 mM NaCl. This result also implies that binding energies of equal magnitude can be obtained at different ionic strengths, for example, 10 and 100 mM, a result clearly inconsistent with eq 1.

The observation of pH_c values always above $pI = 4.9$ for BSA indicates the presence of a positive "patch"[20] in an otherwise negatively charged protein, which makes binding to a strong polyanion such as Hp possible. Although insulin binding occurs both above and below pI (5.7), the maximum in the phase boundary is evident and also suggests ionic strength regimes in which the balance of attractive and repulsive forces differs. Superposition of the two phase boundaries reveals generally larger values of pH_c for Hp, indicating that Hp binds to BSA much more strongly than to insulin, especially at low ionic strengths.

The phase boundaries of Figure 2 provide qualitative indications of nonmonotonic ionic strength dependence. To study effects of ionic strength, I, on binding quantitatively,

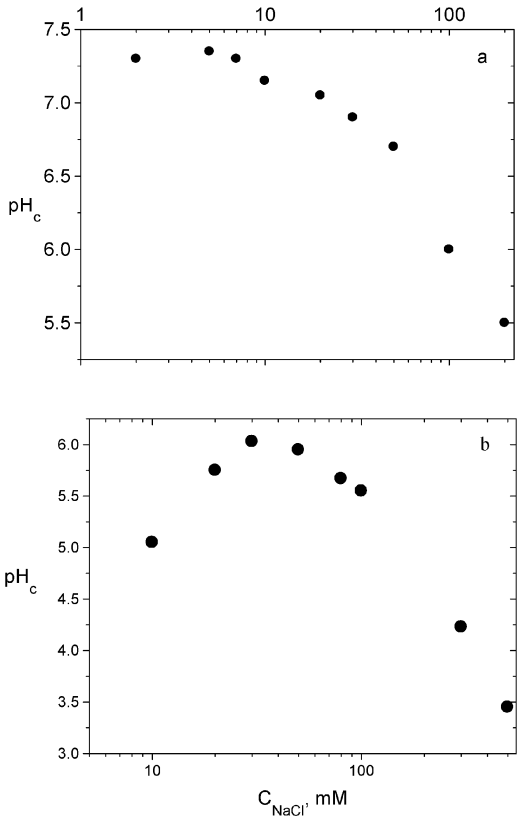

Figure 2. Ionic strength dependence of pH_c for (a) BSA (1 g/L) and Hp (0.1 g/L) and (b) insulin (0.1 g/L) and Hp (0.01 g/L).

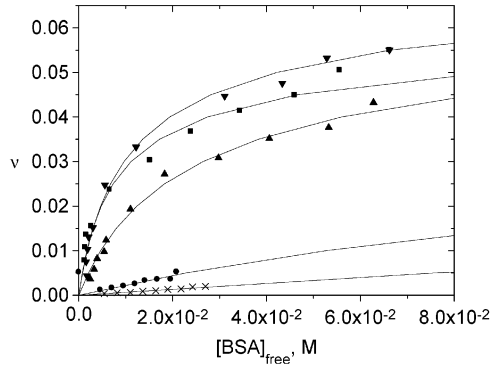

Figure 3. Binding isotherms for BSA and Hp at ionic strengths of (▼) 2, (■) 7, (▲) 10, (●) 30, and (∗) 50 mM in phosphate buffer at pH = 6.8. The solid lines are the curves fitted by the McGhee-von Hippel equation.

FACCE experiments were carried out with BSA-Hp mixtures at various I at pH = 6.8. This pH was chosen to provide binding isotherms over a wide range of I while avoiding adsorption of BSA onto the capillary, which is likely to occur at pH < 6.5. In the resulting binding isotherms shown in Figure 6, ν is defined as the number of bound BSA per charge of Hp because the mass per repeat unit of Hp is not well-defined while the number of charged groups per unit mass can be determined precisely.[14] As seen in Figure 3, the strength of binding as measured by the initial slope of the binding isotherms is seen to increase with decreasing ionic strength but to converge at the lowest ionic strengths.

Additional information can be obtained in the framework of a binding model, such as that of McGhee-von Hippel, which incorporates potential overlap of ligand binding sites

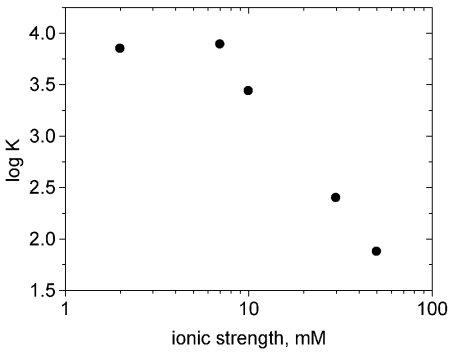

Figure 4. Intrinsic binding constants calculated for BSA-Hp at pH = 6.8 from Figure 3 via the McGhee-von Hippel equation.

and ligand−ligand cooperativity. In this model, a ligand molecule is assumed to bind to the lattice and to cover (i.e., make inaccessible to another ligand) nonconsecutive lattice residues, and ligand−ligand interaction is only allowed between nearest neighbors, bound without intervening free lattice residues.[21] With these assumptions, the equation for noncooperative binding is given as

$$\frac{\nu}{L} = K_{\text{obs}}(1 - n\nu)\left(\frac{1 - n\nu}{1 - (n-1)\nu}\right)^{n-1} \qquad (3)$$

where ν is the number of bound BSA per ionic site of Hp, L is the concentration of free BSA, K_{obs} is the observed binding constant, and n is the binding site size in number of Hp charge groups. Nonlinear curve fitting showed that the binding was well-described by eq 3 without any need for a cooperativity term, leading to the parameters K_{obs} and n. As shown in Figure 4 and as expected from the initial slopes of the isotherms, K_{obs} increases with decreasing ionic strength for $C_{\text{NaCl}} > 10$ mM showing little change at $C_{\text{NaCl}} < 10$ mM, while n varies from 11 to 13 showing a weak tendency to change with ionic strength. The discontinuity in K_{obs} is observed at $I = \sim 10$ mM, at which the plateau was observed in the phase boundary (Figure 2a). These two observations both mean that the same binding energy can exist at two different ionic strengths in the range of low ionic strength. The very large change in binding affinity observed going from ionic strength 10 to 30 mM is a consequence of the transition from the noninteraction domain to the binding domain as can be seen from the phase boundary shown in Figure 2a.

Nonmonotonic behavior is also seen for the binding of β-lactoglobulin (BLG) to the synthetic polyanion polystyrenesulfonate (NaPSS), which displays a maximum in the binding constant at an ionic strength near 20 mM at pH 6.7−7.0, as shown in Figure 5.[10] The dependence of the position of the maximum on ionic strength resembles the observation for lysozyme isoforms,[9] inasmuch as both display a shift to lower I with increase in the protein positive charge. At pH 6.3, the maximum may reside beyond the range of I studied in ref 10.

Despite a linear charge density identical to that of NaPSS, the BLG-binding afffinity is clearly much smaller for PAMPS (sodium (2-acrylamido-2-methylpropanesulfonate)). It has been proposed that NaPSS exhibits hydrophobic properties,[22] but this assertion is controversial because NaPSS

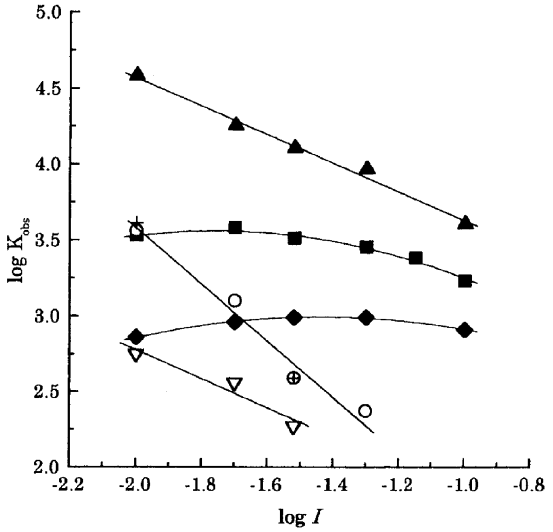

Figure 5. Effect of ionic strength on binding constants of BLG-NaPSS and BLG-PAMPS: (◆) BLG-NaPSS at pH 7.0; (■) BLG-NaPSS at pH 6.7; (▲) BLG-NaPSS at pH 6.3; (▽) BLG-PAMPS (MW = 5.0×10^5) at pH 6.3; (○) BLG-PAMPS (MW = 5.0×10^6) at pH 6.1; (+) BLG-PAMPS (MW = 2.5×10^5) at pH 6.1.[10]

is often considered a paradigm for strong polyelectrolytes. To ascertain whether the nonmonotonic behavior persists when hydrophobic interactions are unambiguously present, studies were carried out with BSA and hydrophobically modified poly(acrylic acid) (HMPAA).

In contrast with the other protein/polymer pairs, BSA and HMPAA form complexes far above p*I*, for example, at pH 8−9.[23,24] At such conditions, the protein charge is about −20 and the polyacid is fully dissociated, so complexation must be primarily hydrophobic, a conclusion also supported by the observation that high MW (150 kD) HMPAAs with more dense degrees of grafting or with longer alkyl side chains bind more BSA at pH 8 whereas the nonalkylated precursors do not bind at all.[24] Typical HMPAA-BSA binding isotherms (Figure 6a,b) show an initial abrupt increase in the number of BSA bound per 1000 acrylic acid units, ν, further binding showing varying anticooperativity features. In the range of 2.5−40 mM Borax, ν increases significantly with buffer concentration, as expected on the basis of the suppression of Coulombic repulsion among proteins or between protein and polyacid. However, at higher *I*, binding decreases markedly and a saturation plateau is rapidly reached at about $\nu = 7$ (Figure 6b).

This nonmonotonic behavior is most clear at high protein concentration, [BSA] > 40 μM, but in the presence of obvious anticooperative association that strongly affects the isotherm slope, while the effect at low [BSA] may be masked by experimental uncertainties and the collection of data at many different [HMPAA]. Therefore, the procedure was modified to limit the fluctuations in both [BSA] and [HMPAA] and thus to facilitate isolation of the effect of salt. From a large volume of BSA/HMPAA solution (w/w ratio of 8 or 16), expected on the basis of the isotherms in Figure 6b to contain less than 10 μM free BSA, aliquots were removed and combined with equal volumes of buffer of varying concentration. The results are shown in Figure 7. Two ionic strength regimes are observed: suppression of

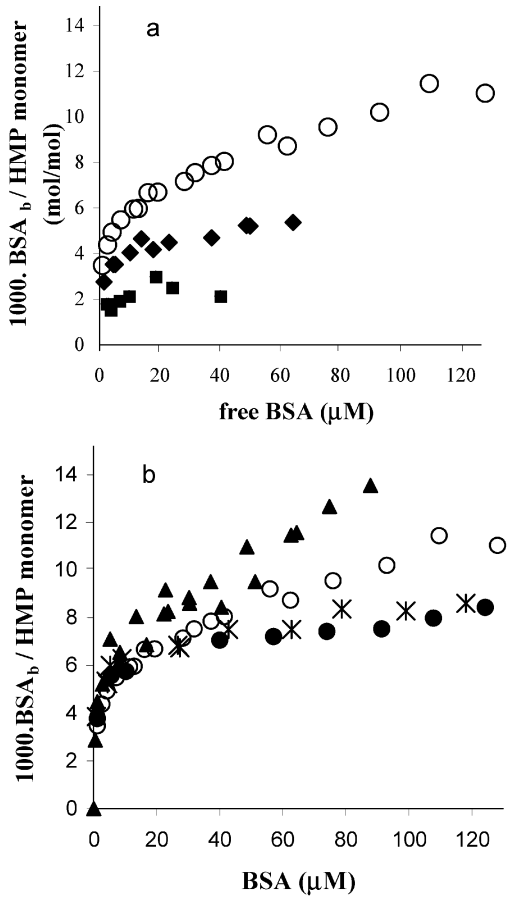

Figure 6. Binding isotherms of BSA onto HMPAA 150-3C18 at pH 9.2 and varying buffer concentration (Borax). The corresponding ionic strengths are the following: (■) 1.875; (◆)7.5; (○) 15; (▲) 30; (∗) 150; (●) 300.

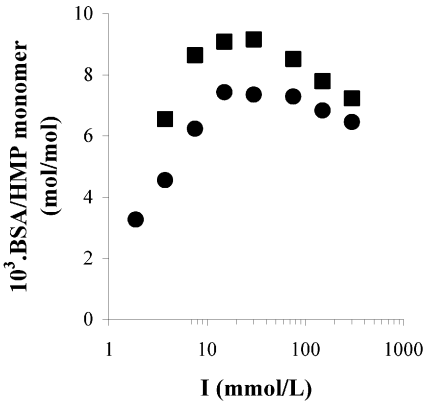

Figure 7. Binding of BSA on HPM 150-3C18 as a function of ionic strength. Sample composition was HMPAA 0.02 wt %, Borax buffer, pH 9.2, BSA/HMPAA (●) 8.1 or (■) 16.3.

binding with increased *I* at *I* > 40 mM and the opposite behavior at low *I* < 10 mM.

Because the salt effects in this case of high pH could arise also from interprotein repulsive interactions, as well as polyacid configurational changes and even multisite attachments of polyacid onto protein, a low MW HMPAA (average degree of polymerization 70, 30× lower than HMPAA 150-C318) was used to limit the binding to one protein per chain. HMPAA 5-3C18, for example, contains on average only two octadecyl groups, below the number of C18/BSA implied by the isotherms of Figure 2b. The nonmonotonic behavior

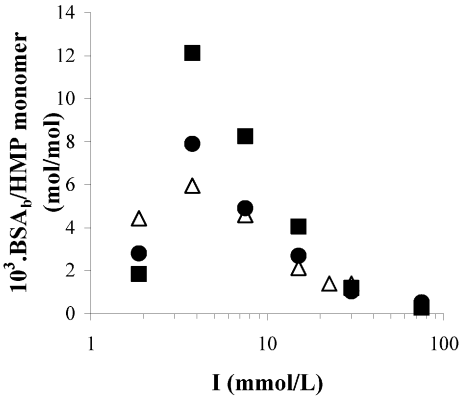

Figure 8. Binding of BSA on HPM 5-3C18 or 5-5C8 as a function of ionic strength. Sample composition was HMPAA 0.02 wt %, Borax buffer, pH 9.2, BSA/5-3C18 (●) 8.1 g/g or (■) 16.3 g/g; BSA/5-5C8 (△) 8.1 g/g.

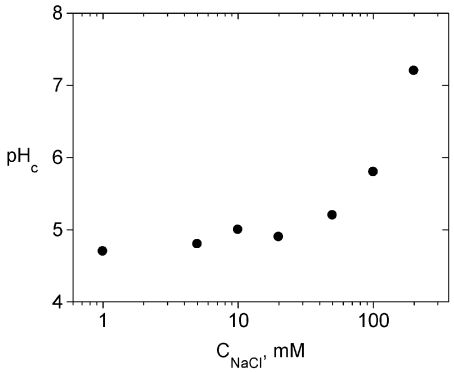

Figure 9. Dependences of pH$_c$ on NaCl concentration of interaction of BSA-PDADMAC from ref 24.

for these low-MW HMPs (Figure 8) appeared even more pronounced than that for high-MW HMPAA. Low MW HMPAA bound very little BSA at any I, presumably reflecting the small number of alkyl groups per polymer, but the binding was dramatically enhanced at $I \approx 4-8$ mM.

Discussion

The phase boundaries of Figure 2 are a qualitative measure of the complex stability, and a diminution of the complex phase area at high salt means that the binding is reduced with increasing I, as expected due to screening of electrostatic attractions. However, when the ionic strength is significantly decreased, the phase boundaries display a plateau or a maximum, corresponding to reduced binding at low ionic strength. This behavior is not unique to polyanions: the phase boundary for the interaction of BSA and the polycation poly(dimethyldiallylammonium chloride) (PDADMAC)[25] in Figure 9 shows that while pH$_c$ tends to increase with increasing C_{NaCl} above 50 mM salt, it is nearly independent of ionic strength below 30 mM, implying that decrease in ionic strength in the low I regime can occur unaccompanied by a change in binding affinity.

Nonmonotonic ionic strength dependence has been seen more dramatically in the binding of lysozyme to two other GAGs, hyaluronic acid (HA) and chondroitin sulfate (CS), which display, as seen in Figure 10, maxima at ca. $I = 20$ and 5−10 mM, respectively.[9] Because the pI of lysozyme

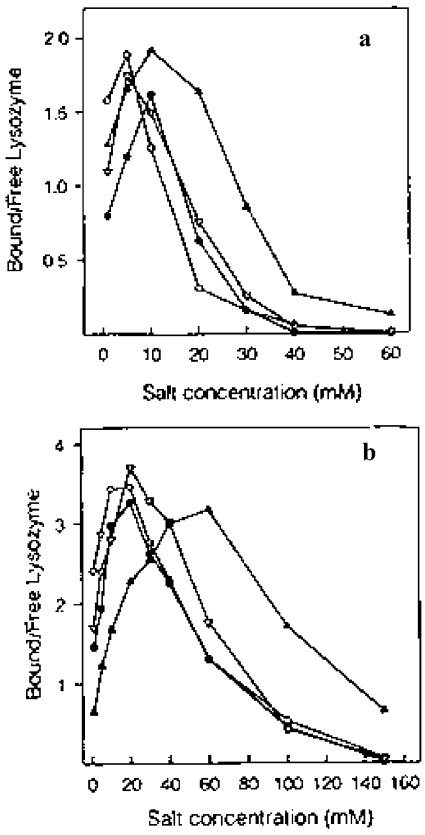

Figure 10. Salt dependence of binding of bovine cartilage lysozyme isoforms at pH = 7.5 (▽, least cationic isoform; ▲, most cationic isoform; ●, pool of all isoforms) and hen egg white lysozyme (○) to (a) chondroitin sulfate-agarose and (b) hyaluronic acid-agarose.[9]

is 11, one sees that the maximum in binding to polyanions is observed not only for (net) anionic proteins with positive charge patches but also for (net) cationic proteins. Figure 10 shows that the most cationic lysozyme isoform exhibits a maximum at a higher ionic strength, demonstrating the influence of the disposition of positive and negative protein charges on the binding behavior.

The dependence of protein binding as a function of ionic strength for HMPAA reveals a subtle relationship between electrostatic and hydrophobic interactions, in which the latter actually amplifies the maximum in binding. This result cannot be attributed to a direct salt effect on the hydrophobic interactions, which are only seen at much higher ionic strengths,[26,27] or to a change in polymer conformation with salt which can be ruled out by the preservation of the maximum in binding observed for low MW polymers with on average two hydrophobes per chain. Because HMPAA is hydrophobically bound to BSA, the modulation of its affinity by changing ionic strength encompasses the entire range of electrostatic contributions, beginning with predominantly repulsive long-range interactions, which diminish association at low I, then passing through a regime of I in which these coexist with attractive interactions between the polyanion and the protein's positive patches, and finally to the predominance of the last at high salt. The high sensitivity to screening suggests that these effects cannot be confused with "salt-bridges"—the pairing of uncompensated charges within low-dielectric and largely anhydrous protein domains. The foregoing considerations argue for the observed salt effects

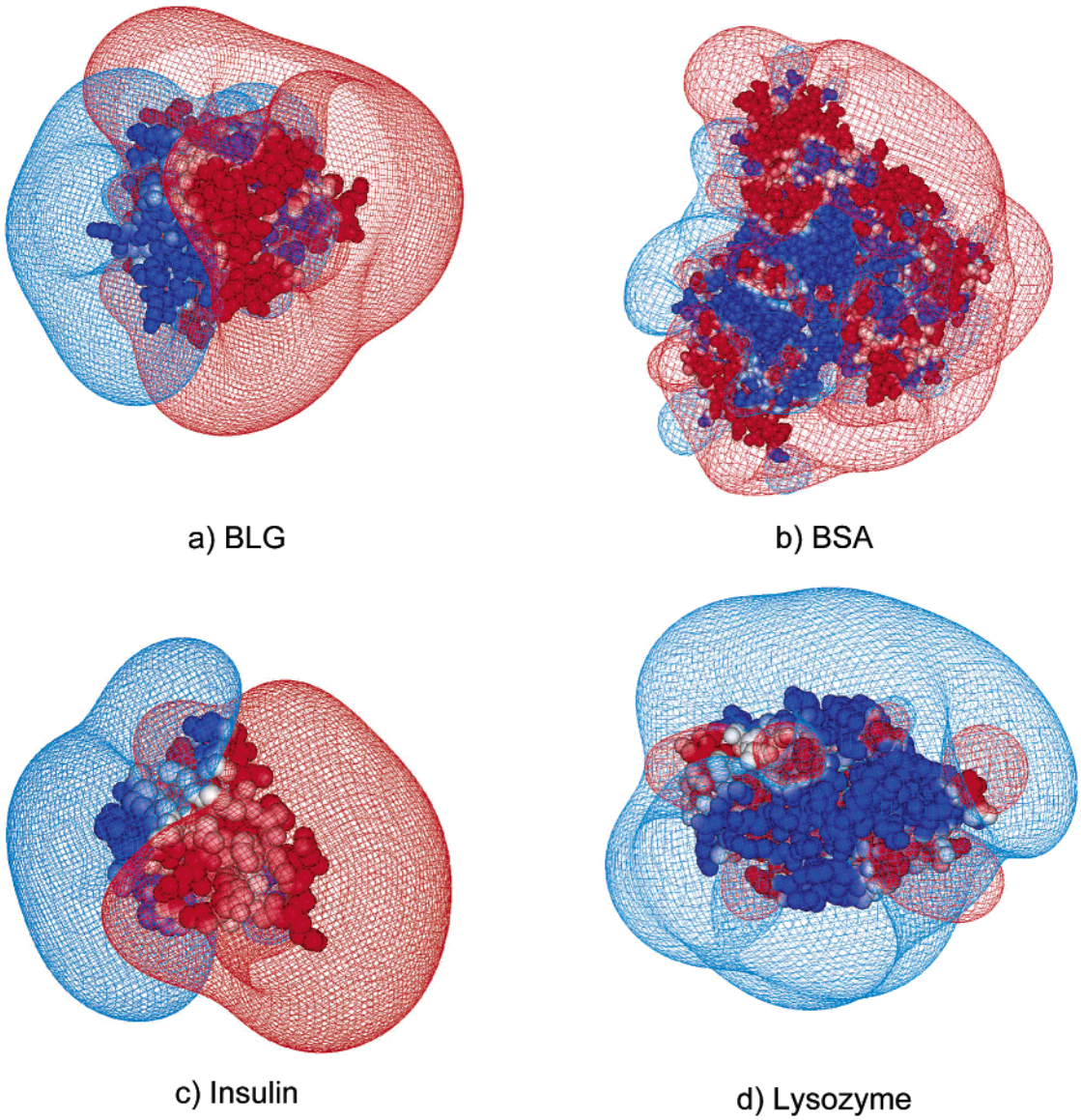

Figure 11. Potential surfaces (−0.1 kT/e (red) and 0.1 kT/e (blue)) around different proteins at pH = 7 and I = 0.15. Potential on protein surface is also colored, blue representing positive and red representing negative potentials.

being similar to those of electrostatic binding and not directly arising from the hydrophobes.

For most of the systems discussed above, binding of the polyelectrolyte is observed "on the wrong side" of the isoelectric point, for example, for polyanions at pH > pI, evidence for interaction of the polyanion with a positive domain or "patch".[10,14,20,28] Hattori et al., following the analysis of Rubinstein and co-workers,[10] showed how treating this anisotropy as a dipole in the case of BLG leads to a maximum in the energy of binding to a polyanion at low ionic strength. Visualization of protein charge is accomplished more realistically via Delphi, as in Figure 11, in which the anisotropies of the potential surfaces for BLG, BSA, insulin, and lysozyme at the same pH and I are displayed. The images portray these proteins as "electrostatically seen" by a polyanion and clearly reveal the dipolar asymmetry of BLG, BSA, and insulin. Binding of the polyanion to the positive domain thus results in a combination of short-range attractive interactions coupled with longer-range repulsive interactions. When the Debye length, $\kappa^{-1} \approx 0.3/\sqrt{I}$ (nm), at high salt is small compared to the protein radius, R_{pro}, all repulsions are screened and the addition of more salt acts to weaken attractions, corresponding to the decrease in affinity with added salt always seen at high I. However, when κ^{-1} is large enough, repulsions become significant, particularly when the protein is predominantly negative as seen in Figure 11a,b,c. The effect of added salt is therefore to screen repulsions thus making association stronger. The boundary between these two regimes is observed near $\kappa^{-1} \approx R_{pro}$, that is, ca. 2−4 nm, corresponding to I = 20−6 mM.

A simplified but more quantitative analysis results from treating the protein as a dipole, as shown in Figure 12. At pH > pI, $Q_- > Q_+$ and the electrostatic binding of the polyanion (q_-) requires $R_+ < R_-$.

The electrostatic interaction energy can be written as the sum of attractive and repulsive terms:[29]

$$U = \frac{q_-}{2\epsilon}\left(Q_- \frac{\exp[-\kappa R_-]}{R_-} - Q_+ \frac{\exp(-\kappa R_+)}{R_+}\right) \qquad (4)$$

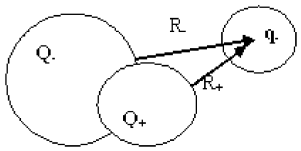

Figure 12. A schematic representation of the interaction of a negatively charged ligand with a protein represented as a dipole $Q_+ < Q_-$.

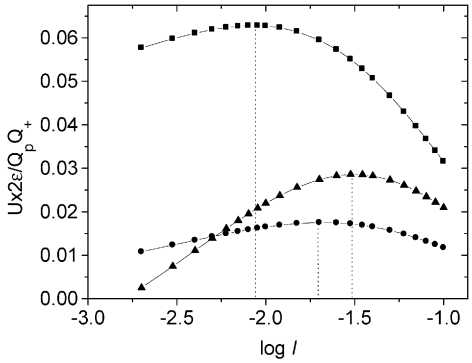

Figure 13. Normalized electrostatic potential energy (calculated via eq 3) vs log I for (■) BSA−Hp ($Q_-/Q_+ = 1.2$, $R_- - R_+ = 0.6$), (▲) BLG-NaPSS ($Q_-/Q_+ = 1.4$, $R_- - R_+ = 0.45$), and (●) insulin-Hp ($Q_-/Q_+ = 1.1$, $R_- - R_+ = 0.2$). Dotted lines show maxima to facilitate comparison with Figures 2b, 4, and 5.

Taking the first derivative of eq 4 with respect to κ and equating it to zero, we find the extremum as

$$\kappa_{max} = -\frac{\ln\left(\frac{Q_+}{Q_-}\right)}{(R_- - R_+)} \qquad (5)$$

corresponding to a maximum in binding energy at a screening length $\kappa^{-1} = -(R_- - R_+)/\ln(Q_+/Q_-)$.

Similarly, a maximum in the binding energy exists for the binding of polyanion to a predominantly negative protein for which $Q_- > Q_+$ and $R_+ < R$. From eq 5, it is possible to estimate the value of κ_{max}, obtaining Q_- and Q_+ as the simple sums of positive and negative amino acids (in the absence of each other) and somewhat arbitrarily (but not unreasonably) setting $R_- - R_+$ on the order of $R_{pro}/6$. For typical values of Q_+/Q_- ranging from 1.2 to 1.5, a maximum in U is expected at $\kappa^{-1} \approx R_{pro}/2$ or $R_{pro}/3$, a value that is valid for any charge located far from the protein, that is, for the charges along the polymer chain that are not in direct contact with the binding site. The results displayed in Figure 13 reveal maxima in normalized interaction energies at exactly the experimentally observed values of I. This success is remarkable given the simplicity of the model with relatively little in the way of adjustable parameters. One obvious refinement would be the use of a configurationally flexible polyelectrolyte chain instead of the simplistic point charge q_- and then consideration of the dependence on the Debye length of the net polyelectrolyte charges near the binding site, but the manifold configurations of the bound polyelectrolyte make this a formidable task. An enhanced model could also be obtained by including additional terms to account for treatment of molecules such as lysozyme, which show multipolar charge distributions. Regardless, the current analysis does demonstrate the merit of considering the dipole-like nature of the protein charge distribution.

According to eqs 4 and 5, maxima should not arise when $Q_+ > Q_-$, but such maxima are nevertheless clearly seen for lysozyme at pH = 7 in Figure 10. Figure 11d shows that lysozyme cannot be considered a dipole but exhibits a higher order of symmetry. We could still expect a similar nonmonotonic behavior for the interaction of this protein with a polyanion when the Debye length is on the order of the distance between the positive and negative domains of the protein. For this situation, however, a correct calculation of electrostatics would require exact location of the multiple domains of like charges on the protein.

While the simple dipole model expressed in eq 4 allows us to obtain the experimental nonmonotonicity with remarkable fidelity, this model clearly lacks the atomistic details of the protein charge distribution that in fact generates the attractive and repulsive force fields. Just as the depictions from Delphi enable us to visualize protein dipoles more realistically, similar visualizations of the variation of electrostatic potential domains with change in ionic strength should help us to understand the nonmonotonic binding behavior. Therefore, negative (−0.1 kT/e) and positive (+0.1 kT/e) electrostatic potential contours around BSA were generated at ionic strengths 0.01, 0.005, and 0.002 and pH = 6.5 (Figure 14).

Figure 2a shows a transition at 10 mM salt from the electrostatic attractive regime dominant at higher I, and we select pH = 6.5 to remain within the regime of net attraction (binding). The selection of 0.1 kT potential surfaces is based on the expectation that the portion of a polyanion chain cooperatively bound to a protein with $R_{pro} = 2-3$ nm would, in the case of Hp, typically comprise about 10 charges, the average number of sulfates and carboxylates for each (ca. 1.2 nm) disaccharide being 3.5.[14] While the position of bound Hp relative to BSA is not precisely known and ideally would be treated statistically, one may imagine Hp avoiding the negative domains for the two higher ionic strengths; but the remarkable expansion of the negative potential domain at the lowest I requires that the Hp chain encounter the influence of the acidic amino acids, thus entering the regime in which added salt screens both attractions and repulsions. This observation points out an important distinction between the binding of chain molecules vs smaller ligands: While some of the polyelectrolyte charges may be tightly bound (within a positive domain, for example), other neighboring polyelectrolyte charges, while subject to statistical fluctuations, are nevertheless locally confined and thus able to sense the dipole nature of the protein.

The parameter q_- in eq 4 represents the array of polyion charges described above. For the simpler case of stiff chains, the number of such polyelectrolyte charges should exhibit a monotonic increase with increasing Debye length, but q_- in eq 4 is essentially unmodified because the distance between the protein and each test charge along the chain is unchanged at the scale of the polymer persistence length: each charge would then exhibit a maximum in electrostatic interaction at similar values of the Debye length. For flexible chains, the problem of specifying the location of polyelectrolyte

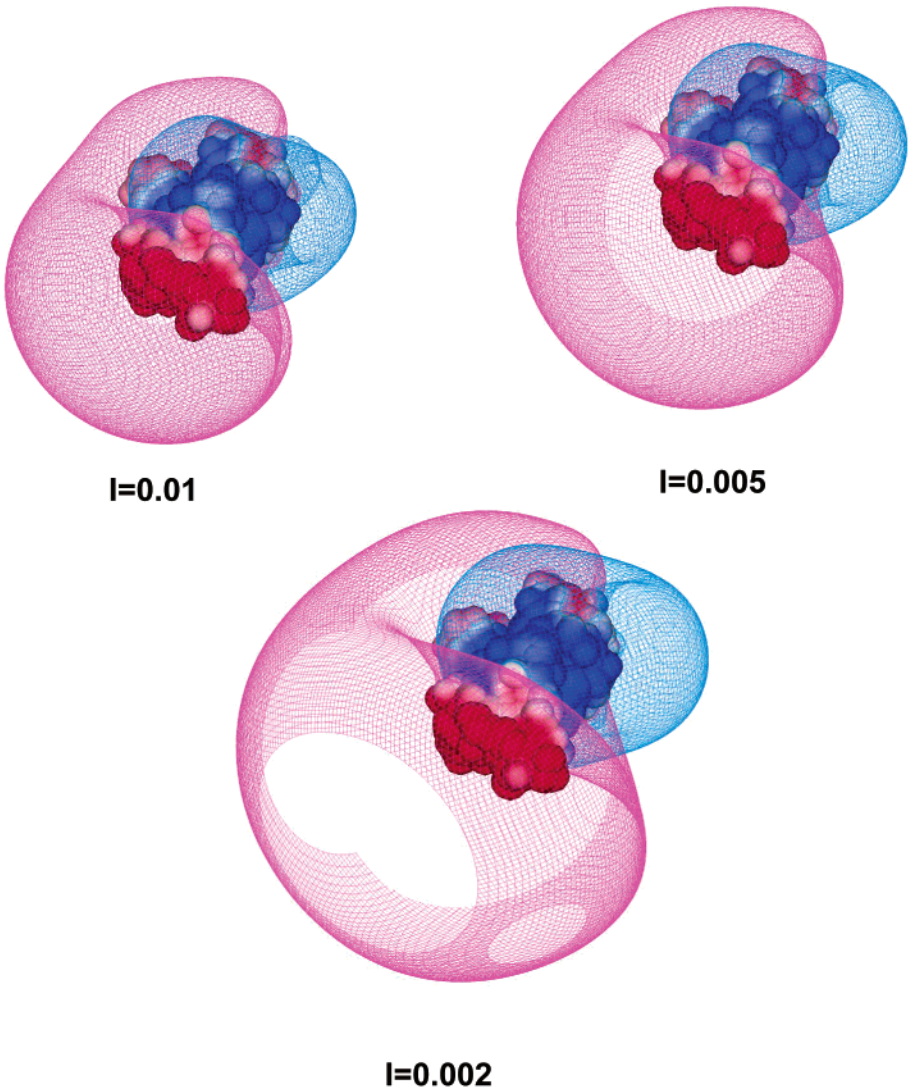

Figure 14. Electrostatic potential contours (−0.1 kT/e (purple) and 0.1 kT/e (blue)) around BSA at different ionic strengths at pH = 6.5. Potentials close to the protein surface (5 Å) are colored blue (positive) and red (negative).

charges is a formidable task, and indeed q_- might increase with a decrease in I because of stronger attraction between protein positive domain and polyion segments or, as argued by Carlsson,[12] might decrease because of chain stiffening. A simple extension of eq 4 is thus not feasible. However, provided that these effects do not dominate, conclusions in terms of nonmonotonic binding energy remain valid.

The extent to which a polyanion can accommodate to the contour of the complementary positive domain is clearly a reflection of chain flexibility. While a rigorous evaluation of the effect of chain flexibility is difficult for the reasons given above, one may compare experimentally flexible chains with stiffer ones such as hyaluronic acid (intrinsic persistence length on the order of 7 ± 2 nm[30,31]). Because such a rigid polymer could not adopt a configuration avoiding repulsive interactions, the repulsive regime would be expected to be more extended, and this is the result seen in Figure 10 in which the repulsive regime is found at $0 < I < 15$ mM for CS but at $0 < I < 60$ mM for HA. The issue of manifold configurations for the bound polyelectrolyte is absent in some related situations, for example, the complex of λ-repressor protein and DNA, for which a crystal structure has been obtained and used to provide fixed locations of all charged groups. For this case, Marky and Manning[11] theoretically showed that salt provided a favorable free energy contribution by screening repulsive interactions between DNA and negative protein groups. Their calculation thus appears to be related to our observations, but there may not be a direct connection because our conventional binding constants imply an initial state of distant separation.[32]

Monte Carlo simulations of polyanions with lysozyme have been carried out by Carlsson et al.,[12] who modeled the protein as charged atoms projected on the surface of a sphere. When only electrostatic forces are considered, a maximum in the number of adsorbed polymer segments appears near 10 mM salt. However, in contrast with experimental findings,[33] these maxima only apply in the case of net positive protein charge, and indeed no binding is observed between polyanions and net negative protein unless a nonelectrostatic interaction is introduced into the model. In the treatment of Carlsson et al., these maxima are a consequence of the stretching of the polyelectrolyte chain at low ionic strength and the concomitant reduction in polymer-protein contacts. At the present time, it is difficult to compare these simulation

results to the maxima observed here in which polyelectrolyte and protein bear the same net charge. However, work currently underway here with the stiff polyanion hyaluronic acid may be illuminating inasmuch as effects of ionic strength on chain stretching should be minimized; in addition, it should be possible to experimentally evaluate the prediction of Carlsson et al. of a shift in the maximum to higher I as protein net charge moves in the direction of polymer charge.

Conclusions

The anisotropy of electrostatic domains around a protein plays a dominant role in determining the ionic strength dependence of its binding to a polyelectrolyte. One consequence is a maximum in polyelectrolyte-protein affinity at ionic strengths corresponding to Debye radii on the order of the protein radius. This condition marks the transition between a region of I dominated by attractions and an ionic strength domain in which repulsions with like-charge protein groups become important. Even when the binding at a specific site is driven by recognition phenomena and short-range forces, association can be strongly modulated by long-range electrostatic effects. The interpretation of complex sensitivity to salt in the presence of a specific (non-Coulombic) association may thus reveal the presence of charge heterogeneity close to the binding site. Inhomogeneous distributions of Coulomb potential at the surface of a protein can thus play a role in tuning the overall affinity by interactions with polymer segments that are not restrictively bound but reside in close vicinity with the protein.

Acknowledgment. We acknowledge support from NSF Grant CHE9987891 (P.L.D.) and NSF/CNRS collaborative research under Grant NSF-9987891/action CNRS-NSF No. 10749. We thank Profs. G.S. Manning, M. Rubinstein, and B. Jonsson for helpful discussions.

References and Notes

(1) Kokufuta, E. *Prog. Polym. Sci.* **1992**, *174*, 647−697.
(2) Dubin, P. L.; Gao, J.; Mattison, K. M. *Sep. Purif. Methods* **1994**, *23*, 1−16.
(3) Griffith, A.; Glidle, A.; Cooper, J. M. *Biosens. Bioelectron.* **1996**, *11*, 625−631.
(4) Muller, M.; Brissova, M.; Rieser, T.; Powers, A. C.; Lunkwitz, K. *Mater. Sci. Eng., C* **1999**, *C8*−*C9*, 163−169.
(5) Manning, G. S. *J. Chem. Phys.* **1969**, *51*, 924−933.
(6) Record, M. T.; Anderson, C. F.; Lohman, T. M. *Q. Rev. Biophys.* **1978**, *2*, 103−178.
(7) Fried, M. G.; Stickle, D. F. *Eur. J. Biochem.* **1993**, *218*, 469−475.
(8) Singer, P. T.; Wu, C. W. *J. Biol. Chem.* **1988**, *263*, 4208−4214.
(9) Moss, J. M.; VanDamme, M. P.; Murphy, W. H.; Preston, B. N. *Arch. Biochem. Biophys.* **1997**, *348*, 49−55.
(10) Hattori, T.; Hallberg, R.; Dubin, P. L. *Langmuir* **2000**, *16*, 9738−9743.
(11) Marky, N. L.; Manning, G. S. *J. Am. Chem. Soc.* **2000**, *122*, 6057−6066.
(12) Carlsson, F.; Linse, P.; Malmsten, M. *J. Phys. Chem. B* **2001**, *105*, 9040−9049.
(13) Mattison, K. M.; Wang, Y.; Grymonpre, K.; Dubin, P. L. *Macromol. Symp.* **1999**, *140*, 53−76.
(14) Hattori, T.; Kimura, K.; Seyrek, E.; Dubin, P. L. *Anal. Biochem.* **2001**, *158*, 158−167.
(15) Tanford, C.; Kirkwood, J. G. *J. Am. Chem. Soc.* **1957**, *79*, 5333−5339.
(16) Tanford, C.; Wagner, M. L. *J. Am. Chem. Soc.* **1954**, *76*, 3331−3336.
(17) Tanford, C.; Epstein, J. *J. Am. Chem. Soc.* **1954**, *76*, 2163−2169.
(18) Tanford, C.; Swanson, S. A.; Shore, W. S. *J. Am. Chem. Soc.* **1955**, *77*, 6414−6421.
(19) Tanford, C.; Bunville, L. G.; Nozaki, Y. *J. Am. Chem. Soc.* **1959**, *81*, 4032−4036.
(20) Park, J. M.; Muhoberac, B. B.; Dubin, P. L.; Xia, J. *Macromolecules* **1992**, *25*, 290−295.
(21) McGhee, J. D.; von Hippel, P. H. *J. Mol. Biol.* **1974**, *86*, 469−489.
(22) Mori, S.; Oosaki, T. *ACS Symp. Ser.* **1996**, *635*, 347−350.
(23) Tribet, C.; Porcar, I.; Bonnefont, P. A.; Audebert, R. *J. Phys. Chem. B* **1998**, *102*, 1327−1333.
(24) Porcar, I.; Gareil, P.; Tribet, C. *J. Phys. Chem. B* **1998**, *102*, 7906−7909.
(25) Kaibara, K.; Okazaki, T.; Bohidar, H. B.; Dubin, P. L. *Biomacromolecules* **2000**, *1*, 100−107.
(26) Shaltiel, S. *Methods Enzymol.* **1974**, *34*, 126−140.
(27) Shaltiel, S.; Halperin, G. *Proc. FEBS Meet.* **1979**, *52*, 441−451.
(28) Grymonpre, K. R.; Staggemeier, B. A.; Dubin, P. L.; Mattison, K. M. *Biomacromolecules* **2001**, *2*, 422−429.
(29) Bowman, W. A.; Rubinstein, M.; Tan, J. S. *Macromolecules* **1997**, *30*, 3262−3270.
(30) Hayashi, K.; Tsutsumi, K.; Norisuye, T.; Teramoto, A. *Polym. J.* **1996**, *28*, 922−928.
(31) Ghosh, S.; Li, X.; Reed, C. E.; Reed, W. F. *Biopolymers* **1990**, *30*, 1101−1112.
(32) Manning, G. S. Private communication.
(33) Xia, J.; Dubin, P. L.; Kim, Y.; Muhoberac, B. B.; Klimkowski, V. J. *J. Phys. Chem.* **1993**, *97*, 4528−4534.

BM025664A